Photoacoustic Excitation of the Interior Surface of an Acoustic Resonator for Speed of Sound Measurement[1]

G. Benedetto[2], R. M. Gavioso[2], and R. Spagnolo[2,3]

---

[1] Paper presented at the Thirteenth Symposium on Thermophysical Properties, June 22-27, 1997, Boulder, Colorado, U.S.A.

[2] Istituto Elettrotecnico Nazionale Galileo Ferraris, Acoustics Department, Strada delle Cacce 91, 10135 Torino, Italy.

[3] To whom correspondence should be addressed.

ABSTRACT

A remote optical technique is proposed as a valid alternative to conventional electroacoustic excitation of sound inside an acoustic resonator. Efficient photoacoustic conversion of an amplitude-modulated light beam, impinging on the interior solid surface of the resonator wall, into a stationary acoustic field, is achieved. The reported results were obtained in a cylindrical stainless steel resonator of about 572 cm^3 ; the radiation source is the 514 nm line of an Ar^+ laser. The laser beam can be focused on different points of the resonator internal surface. The signal frequency dependence is well interpreted in terms of gas-microphone detection theory. The precision obtained in the measurement of resonance frequency f_N and halfwidth g_N of the cavity modes is in the order of 10^{-6} of f_N and is likely to be further improved by minor refinements of the experimental apparatus.

KEY WORDS: photoacoustic effect; acoustic resonator; speed of sound

1. INTRODUCTION

Acoustic resonators are at present the most reliable and accurate tools for measuring the speed of sound in pure gases and mixtures [1, 2]. The basic principle of the measurement is the determination of a number of resonance frequencies in the cavity, in the presence of a stationary acoustic field. Traditionally the source and the detector are electroacoustic transducers, typically condenser microphones mounted flush with the internal surface of the resonator; these perturb resonance frequencies in a minor and predictable way. Nevertheless these transducers are limited in their use in hostile environments, like in presence of corrosive gases and at low and high working temperatures. These kind of difficulties are sometimes overcome using remote transducers operated at room temperatures and separated from the test gas through diaphragms and waveguides [3]. An attractive alternative consists in experimenting remote optical techniques that do not require physical transducers in contact with the measurement environment. The results reported in this paper show that the source transducer can be successfully substituted by a photoacoustic source generated focussing an amplitude modulated laser beam directly on the resonator wall without appreciable reduction of measurement precision.

In the following sections the experimental configuration is described and source characteristics are illustrated and discussed in terms of their suitability for application in speed of sound measurements.

2. EXPERIMENTAL APPARATUS

The resonator is a gastight, stainless steel (type 304), cylindrical resonator, ~ 90 mm in diameter and length. The resonator was initially designed to study photoacoustic excitation of (argon + NO_2) mixtures and is described in detail elsewhere [4]; some minor modifications were introduced to set up present experimental configuration: two adapters are machined midway between the cylinder ends, 90° apart from each other on the azimuthal coordinate, to accept respectively the electroacoustic detector (a 1/4" condenser microphone) and a glass window. A schematic representation of the optical path is shown in Fig. 1. The laser beam (Ar^+, 514 nm) passes through an acousto-optical modulator driven by a waveform synthetizer; the modulated component enters into the cavity through the window and impinges on the stainless steel head of the gas inlet valve, while the continuos one is reflected on a photodiode which allows control of incident power stability. The valve head, 3 mm in diameter, is machined flush with the interior surface of the resonator and black-painted to enhance optical energy absorption and also to reduce scattering; a bi-convex lens allows to adjust the diameter of the light spot on its surface in order to achieve its uniform illumination.

Standard lock-in recovery of the detector microphone signal and measurement procedures are adopted [4]. The resonator was thermally insulated to reduce temperature fluctuations, nevertheless during the time necessary to record one resonance curve (~ 6

min), temperature shifts were in the order of 5 mK; the technique would be improved using an optical fiber in order to make possible speed of sound measurements inside a thermostat.

3. PERFORMANCE TESTS

3. 1 Sound production mechanism

In the original experimental photoacoustic geometry, the sample is enclosed in a cell filled with a nonabsorbing gas. The sample is illuminated by amplitude modulated monochromatic light. Periodic heat flow between the sample and the gas causes a periodic pressure variation in the gas. Only a thin layer of gas adjacent to the surface of the solid responds thermally to the periodic heat flow and can be regarded as a vibrating piston creating the acoustic signal detected in the cell. The thickness of this layer is confined to the gas thermal diffusion length:

$$\mu_g = \left(\frac{k_g}{\pi f \rho_g C_g}\right)^{0.5} \qquad (1)$$

where k_g , ρ_g and C_g are respectively the thermal conductivity, mass density and isochoric specific heat of the gas and f is the modulation frequency. A simple one-dimensional model [5], suitably interpreted, gives expression for the generated signal which are substantially correct in most experimental configurations. The theory develops a solution for the heat diffusion equation in the solid sample and the surrounding gas imposing boundary conditions of temperature and heat-flux continuity at their separation interface.

Considering the stainless steel optical absorption coefficient β and the optical absorption length $\mu_\beta=\beta^{-1}$, the resonator wall can be considered an optically and thermally

thick sample, as its thickness l is such that: $l >> \mu_S >> \mu_\beta$, where μ_S is the steel thermal diffusion length. In this case the spatially averaged temperature θ of the gas within the boundary layer can be determined as a function of incident light intensity I and thermal diffusion length μ_s and thermal conductivity k_s of the solid [5]:

$$\theta \approx I \frac{\mu_s}{k_s} \tag{2}$$

The periodic displacement of the gas piston can be simply estimated using the ideal gas law and found to be:

$$\delta x = \frac{\mu_g}{\sqrt{2}} \frac{\theta}{T} \tag{3}$$

where T is the ambient temperature. Periodic thermal expansion of the sample (the acoustic mode) can also give a minor contribution to the gas pressure variation but the corresponding displacement of the solid surface in our experimental configuration can be calculated to be four orders of magnitude lower than that expressed in eq.(3).

Assuming that the rest of the gas contained in an acoustic resonator responds adiabatically to the action of this photoacoustic piston placed in $\boldsymbol{r}_0$, the acoustic pressure at the position $\boldsymbol{r}$ inside the cavity can be evaluated as a function of the cavity normal modes, whose corresponding eigenfunctions and eigenvalues are Φ_N and K_N [1]:

$$p_\omega(\boldsymbol{r}|\boldsymbol{r}_0) = i\omega\rho_g S_\omega \sum_N \frac{\Phi_N(\boldsymbol{r},\omega)\Phi_N(\boldsymbol{r}_0,\omega)}{V\Lambda_N\left[K_N^2(\omega) - k^2\right]} \tag{4}$$

where V is the resonator volume, Λ_N is a normalization constant, $\omega = 2\pi f$, k is the sound propagation constant and S_ω is the source strength:

$$S_\omega = 4\pi a^2 \omega \ \delta x \tag{5}$$

where a is the laser beam radius. If only one mode is excited in the resonator, use of expressions (1-5) allows calculation of the amplitude of a photoacoustically excited resonance at the position of the detector microphone. Fig.2 shows the experimentally determined dependence on incident power of the amplitude of the first pure radial mode (001) when the resonator is filled with argon at 100 kPa near ambient temperature; the photoacoustic source efficiency shows its linearity over nearly one order of magnitude of incident power. Incidentally this result can be used to infer a value of thermal effusivity e_S of the solid on which photoacoustic conversion takes place, through the proportionality factor between light intensity and average temperature of the gas vibrating piston:

$$e_S = \sqrt{k_s \rho_s C_s} \tag{7}$$

where ρ_s and C_s are respectively the density and the specific heat of the solid. Regression analysis of results reported in Fig.2 gives a value for e_S equal to $7.4 \cdot 10^3$ $W \cdot s^{0.5} \cdot m^{-2} \cdot K^{-1}$ which agrees within 10 % with the value [6] of type 304 stainless steel, the difference being probably due to the thermal influence of the black-paint. This result gives a qualitative and quantitative proof of the validity of the above illustrated model.

3.2 Frequency dependence

In the case of an optically and thermally thick sample, gas-microphone theory [5] gives an approximated expression for the average acoustic pressure generated in a photoacoustic cell of length L filled with gas at a static pressure P:

$$\delta p \approx \frac{1-i}{2} \ \mu_g \ \frac{\mu_s}{k_s} \frac{\gamma P I}{2\sqrt{2} L T} \tag{6}$$

where γ is the gas specific heat ratio; it is evident from eq. (6) that the acoustic signal does not depend on β and varies as f^{-1} through the product $\mu_g \cdot \mu_s$. In Fig. 3 are shown photoacoustic signal dependencies on frequency, experimentally determined in a conventional small volume photoacoustic cell (1.5 cm^3). The curves are relative to a "naked" steel sample and a black-painted one. Expected frequency dependence (f^{-1}) is well confirmed for the first sample, while the second shows a slightly different frequency behavior ($f^{-0.8}$); this is not surprising as it can be justified by the stratified nature of the sample. In Fig. 4 is illustrated the signal photoacoustically excited in the large volume cylindrical resonator in the same frequency range; again this is found to depend on frequency as $f^{-0.8}$, in agreement with the hypothesis that the heuristic model illustrated above is substantially correct.

3.3 Selectivity of modes

A not negligible advantage of the optical nature of the photoacoustic excitation is that it can be used to generate sound in different positions inside the resonator; this facility would be particularly useful in avoiding effects of overlapping between adjacent modes of different symmetry. This assertion is confirmed in Fig. 5, where are compared the calculated and experimental efficiency of the source in exciting the second purely longitudinal mode (002) as a function of longitudinal coordinate of source position on the resonator wall.

3.4 Precision

In order to measure resonance frequencies f_N and half-widths g_N , standard procedures were adopted [2]. Resonances were recorded sweeping frequency through f_N at

11 discrete points in steps of $g_N/5$. At each frequency, the in phase and quadrature voltages produced by the detector were measured. The 11 frequencies and 22 voltages where fit with a complex function with 8 parameters [7]; the complex background terms in this function, are also suitable to keep into account the frequency dependence of the source efficiency, as it was tested with experimental and synthetized data. Resonance curves were recorded for several modes of different symmetry in argon in the pressure range (10÷500) kPa. At ambient pressure measured voltages typically fit to the best determined function with a precision better than 0.2% of maximum voltage; it follows that f_N is determined by the fit with a precision of 0.2% of g_N , that is 10^{-6} of f_N The effect of the signal declining as $p^{-1.5}$ and the effect of the resonance half-widths increasing as $p^{-0.5}$ reduce frequency resolution at lower pressure. At all pressures the signal-to-noise ratio is a factor 2 worse than that characteristic of an electroacoustic source in similar experimental conditions; the difference is attributed to laser power instability whose relative fluctuations have been measured to be in the order of 0.1%.

As an example Fig. 6a,b reports fitted voltages, and corresponding normalized deviations for mode (001) at 100 kPa near ambient temperature. This precision is enough for routine measurements of speed of sound and it would be further improved of an order of magnitude in a spherical resonator as a consequence of reduced resonance half-widths.

CONCLUSIONS

Reported results show that photoacoustic effect in solids can be a valid alternative to electroacoustic excitation in measurements of speed of sound in hostile environment.

Future perspectives include investigation of the possibility to substitute also the detector transducer by means of an optical detection technique; the most promising approach seems to be the optical beam deflection signal produced by the movement of a metallic diaphragm facing the acoustic field inside the resonator.

REFERENCES

1. J.P.M. Trusler, *Physical Acoustics and Metrology of Fluids* (IOP Publishing Ltd, Bristol, 1991).
2. M.R.Moldover, J.B. Mehl, and M. Greenspan, J. Acoust. Soc. Am. 79: 253 (1986).
3. K.A. Gillis, M.R. Moldover, and A.R.H. Goodwin, Rev. Sci. Instrum. **62**: 2213 (1991)
4. G. Benedetto, M.R. Gavioso, and R.Spagnolo, in Proceedings of *IEEE Instrumentation and Measurement Technology Conference* (Brussels, Belgium, June 4-6, 1996) p. 257.
5. A.Rosencwaig and A. Gersho, J. Appl. Phys. **47**: 64 (1976).
6. *Handbook of Tables for Applied Engineering Science*, 2nd Edition, R.E. Bolz and G.L. Tuve, eds. (CRC Press, Boca Raton, Florida, 1976), p. 118.
7. J.B. Mehl, J. Acoust. Soc. Am. **64**: 1523 (1978).

FIGURE CAPTIONS

Fig. 1. Block diagram and cross-section of the cylindrical resonator showing details of optical excitation set-up.

Fig. 2 Amplitude of the first pure radial mode at 100 kPa near ambient temperature, as a function of incident power.

Fig.3. Frequency dependence of the signal generated in a conventional photoacoustic cell.

Fig. 4. Frequency dependence of photoacoustic signal in the cylindrical resonator.

Fig. 5. Comparison between calculated and experimental dependence of mode (200) amplitude as a function of longitudinal position of the photoacoustic source.

Fig. 6a. In-phase (solid curve) and quadrature (dashed curve) voltages from the detector as a function of frequency near the (001) resonance in argon at 100.1 kPa, 294.37 K.

Fig. 6b. Difference between measured and calculated voltages with fitted parameters from complex Lorentzian plus background function [7].

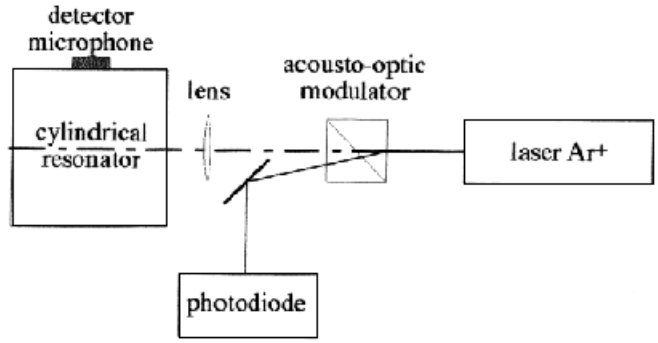
detector
microphone
cylindrical
resonator
lens
acousto-optic
modulator
laser Ar+
photodiode

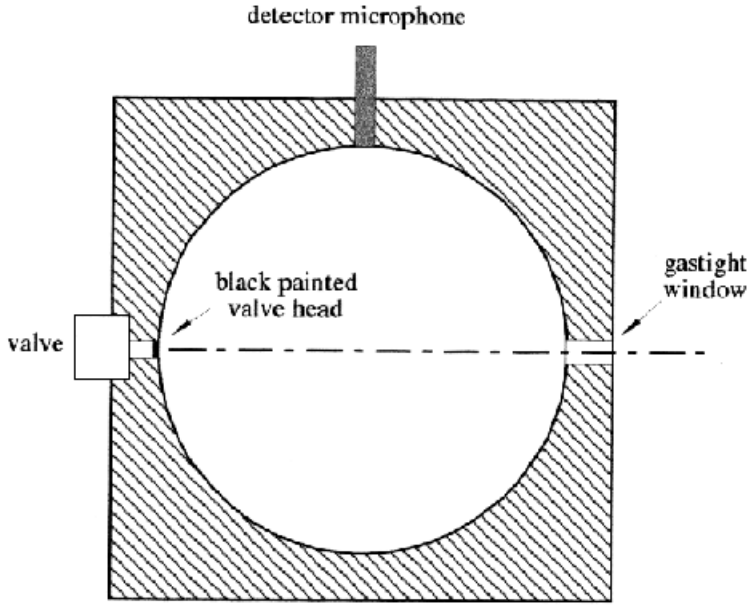
detector microphone
black painted
valve head
gastight
window
valve

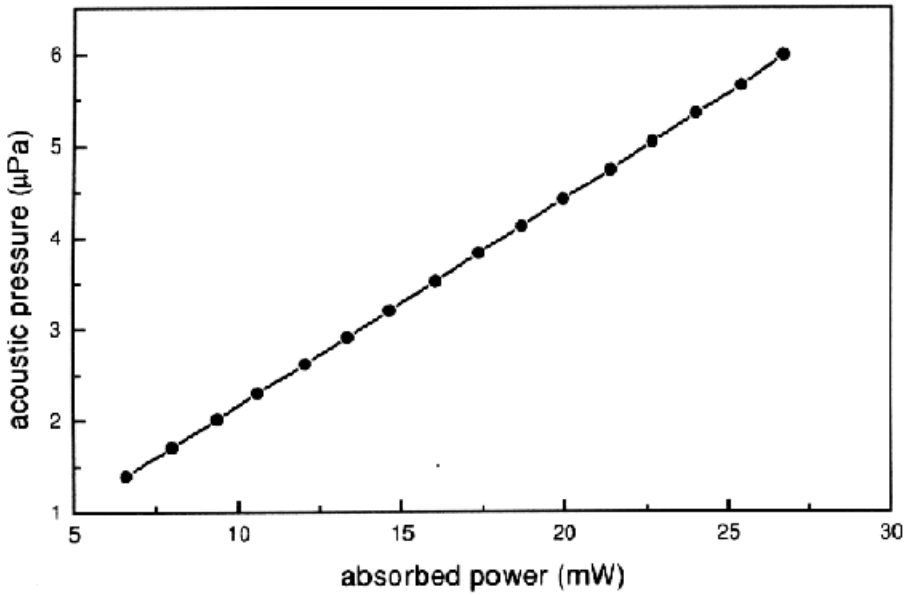
acoustic pressure (μPa)
1
2
3
4
5
6
5
10
15
20
25
30
absorbed power (mW)

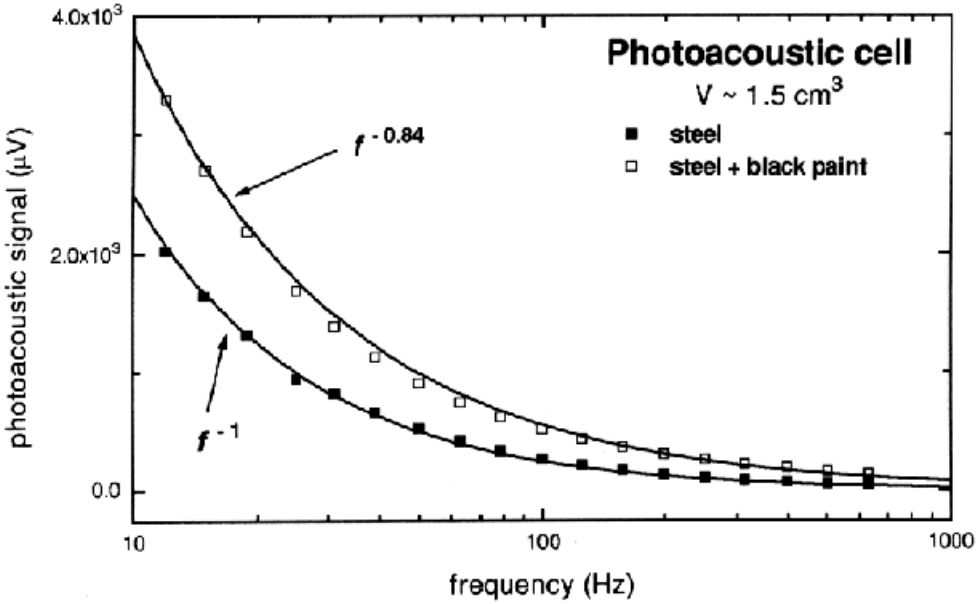
Photoacoustic cell
V ~ 1.5 cm3
steel
steel + black paint
f - 0.84
f - 1
4.0x10^3
2.0x10^3
0.0
10
100
1000
photoacoustic signal (μV)
frequency (Hz)

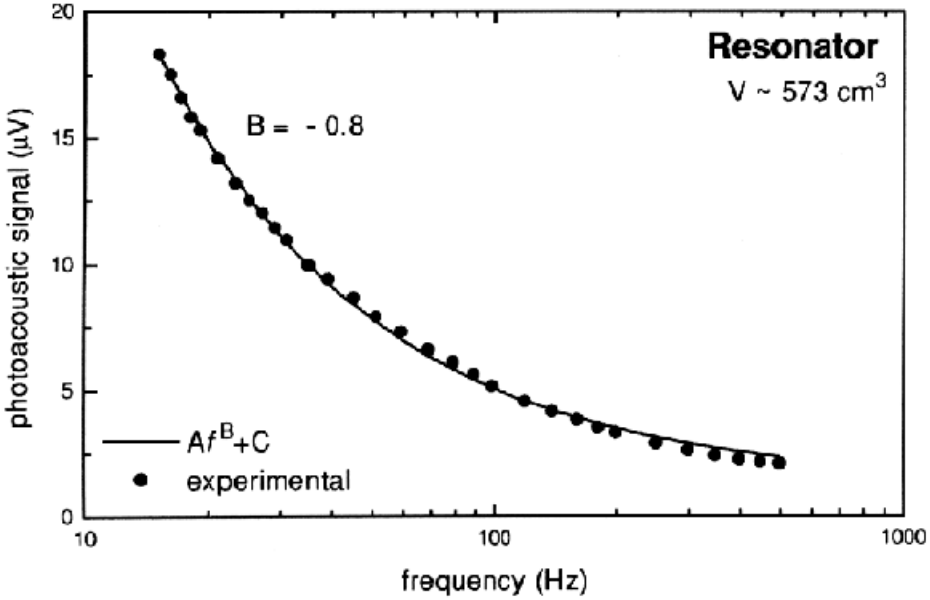
Resonator
V ~ 573 cm3
B = - 0.8
Af^B+C
experimental
photoacoustic signal (μV)
frequency (Hz)
20
15
10
5
0
10
100
1000

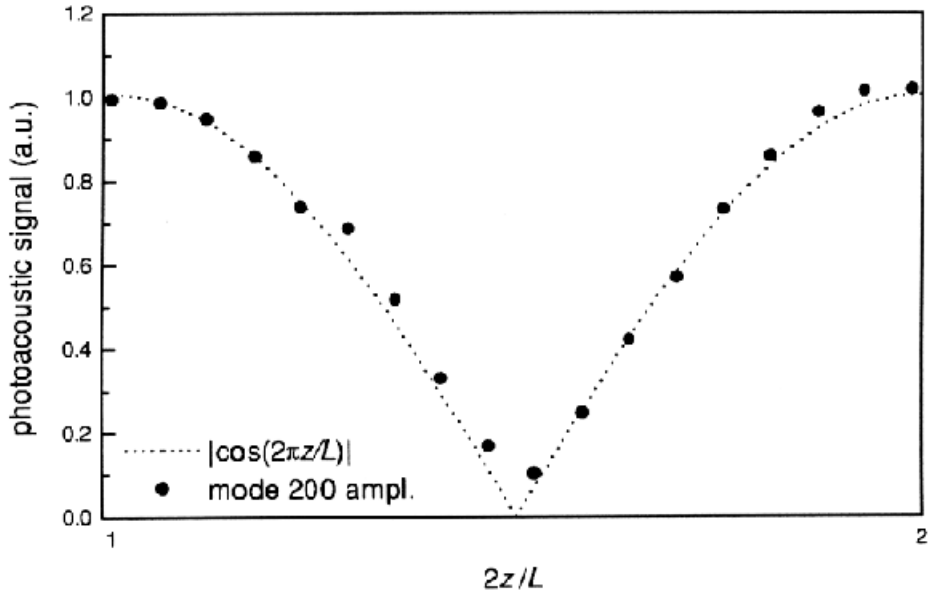
1.2
1.0
0.8
0.6
0.4
0.2
0.0
photoacoustic signal (a.u.)
|cos(2πz/L)|
mode 200 ampl.
1
2
2z/L

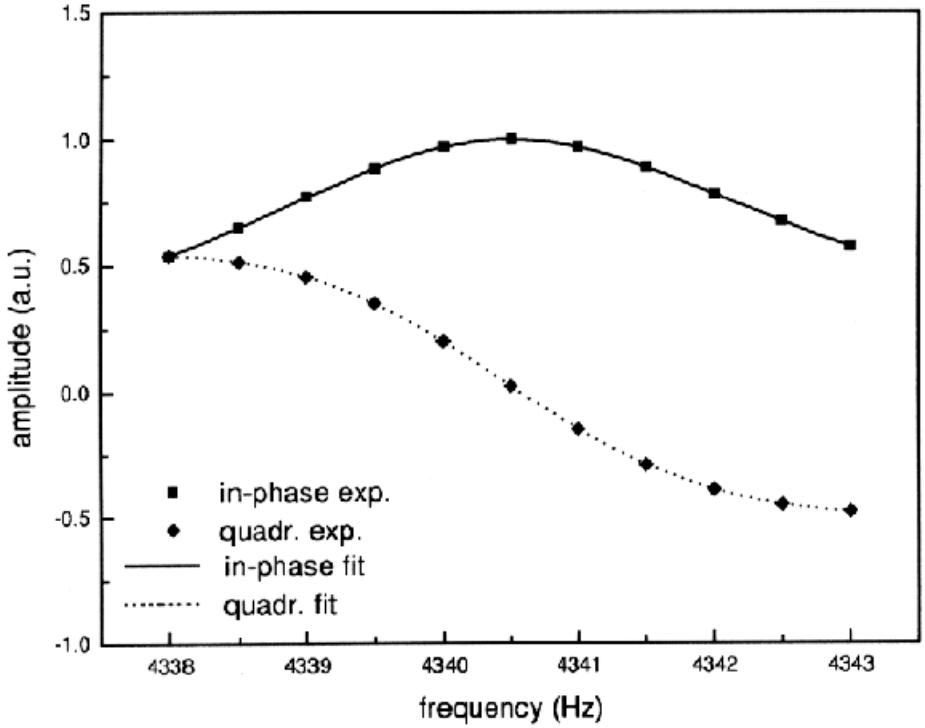
1.5
1.0
0.5
0.0
-0.5
-1.0
amplitude (a.u.)
4338
4339
4340
4341
4342
4343
frequency (Hz)
in-phase exp.
quadr. exp.
in-phase fit
quadr. fit

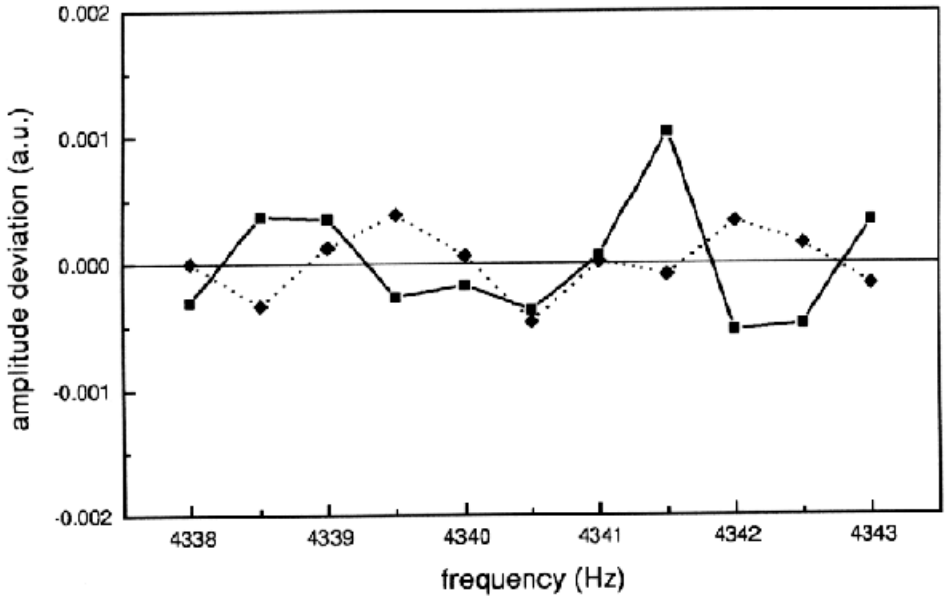
0.002
0.001
0.000
-0.001
-0.002
amplitude deviation (a.u.)
4338
4339
4340
4341
4342
4343
frequency (Hz)